

Article

A New Approach to COVID-19 Detection: An ANN Proposal Optimized through Tree-Seed Algorithm

Muhammet Fatih Aslan ^{1,*} , Kadir Sabanci ¹  and Ewa Ropelewska ² 

¹ Department of Electrical and Electronics Engineering, Karamanoglu Mehmetbey University, Karaman 70100, Turkey; kadirSabanci@kmu.edu.tr

² Fruit and Vegetable Storage and Processing Department, The National Institute of Horticultural Research, Konstytucji 3 Maja 1/3, 96-100 Skierniewice, Poland; ewa.ropelewska@inhort.pl

* Correspondence: mfatihhaslan@kmu.edu.tr; Tel.: +90-541-438-5285

Abstract: Coronavirus disease (COVID-19), which affects the whole world, continues to spread. This disease has infected and killed millions of people worldwide. To limit the rate of spread of the disease, early detection should be provided and then the infected person should be quarantined. This paper proposes a Deep Learning-based application for early and accurate diagnosis of COVID-19. Compared to other studies, this application's biggest difference and contribution are that it uses Tree Seed Algorithm (TSA)-optimized Artificial Neural Networks (ANN) to classify deep architectural features. Previous studies generally use fully connected layers for end-to-end learning classification. However, this study proves that even relatively simple AlexNet features can be classified more accurately with the TSA-ANN structure. The proposed hybrid model provides diagnosis with 98.54% accuracy for COVID-19 disease, which shows asymmetric distribution on Computed Tomography (CT) images. As a result, it is shown that using the proposed classification strategy, the features of end-to-end architectures can be classified more accurately.



Citation: Aslan, M.F.; Sabanci, K.; Ropelewska, E. A New Approach to COVID-19 Detection: An ANN Proposal Optimized through Tree-Seed Algorithm. *Symmetry* **2022**, *14*, 1310. <https://doi.org/10.3390/sym14071310>

Academic Editors: Kóczy T. László and István A. Harmati

Received: 28 May 2022

Accepted: 22 June 2022

Published: 24 June 2022

Publisher's Note: MDPI stays neutral with regard to jurisdictional claims in published maps and institutional affiliations.



Copyright: © 2022 by the authors. Licensee MDPI, Basel, Switzerland. This article is an open access article distributed under the terms and conditions of the Creative Commons Attribution (CC BY) license (<https://creativecommons.org/licenses/by/4.0/>).

Keywords: ANN; AlexNet; COVID-19; transfer learning; TSA

1. Introduction

The SARS-CoV-2 virus, which emerged in 2019, affected the whole world and is still an ongoing problem all over the world [1,2]. Although it is proclaimed by the World Health Organization (WHO) that the mortality rate of the virus is lower than other coronaviruses, the high spread rate of the virus obligated the WHO to declare the virus, also called COVID-19, as a pandemic on 11 March 2020 [3–5]. Due to the contagious effect of COVID-19, curfews were imposed in many countries and social life was restricted. Because of this restriction, people spent more time at home and used social media platforms more intensively [6]. Worldwide, from 8 December 2020 to the present (10 June 2022), more than 530 million people have been infected and 6.3 million deaths have occurred due to COVID-19 [7]. Fever, dry cough, loss of appetite, and fatigue are the most common symptoms of COVID-19. In some cases it is possible to encounter liver injury, septic shock, and pneumonia [8].

The main diagnostic approaches in COVID-19 today are generally real-time Reverse Transcription Polymerase Chain Reaction (rRT-PCR), chest Computed Tomography (CT) imaging, X-ray imaging, etc. [9]. The rRT-PCR is a method that reveals the presence of a specific genetic sequence in a pathogen which can be a virus. The most important advantage of this method is the ability to create an almost instant result. Therefore, the rRT-PCR test is the most-used diagnostic method to detect COVID-19 [10]. However, the percentage of rRT-PCR positives in throat swab samples is reported as roughly 30–60% because of limitations in sample collection, kit performance and transportation [11,12].

The most common alternative to rRT-PCR is chest Computed Tomography (CT) imaging. CT images of different angles of the chest area are used for COVID-19 diagnosis. This

method has better sensitivity in COVID-19 diagnosis than rRT-PCR tests [9,12]. Unlike the rRT-PCR test, CT imaging does not need any extra equipment over hospital equipment. Although the CT imaging method has many advantages as mentioned above, the main disadvantage of the CT imaging method is that professional personnel are required for the interpretation of CT images [13]. Although this need can be easily met under normal conditions, the heavy workload of specialist doctors can cause problems in pandemic conditions. All healthcare professionals are also under a heavy workload, as the COVID-19 pandemic is causing significant constraints on healthcare systems around the world [14].

Recently, Artificial Intelligence (AI), which represents a symmetrical imitation of the human brain, is becoming more capable in many areas including medical imaging tasks such as CT imaging, MR imaging, and X-ray imaging [13]. In literature, AI has been employed for various tasks such as bone age determination, COVID-19 diagnosis, abnormal problems in the chest or tuberculosis detection etc. [15–17]. Deep Learning (DL), which is the trend application of artificial intelligence today, is now successfully used in many medical diagnostic applications due to the huge amount of data available. One of the most important features of DL is that it processes big data efficiently. It also eliminates the need to manually extract image features. In this respect, it provides superiority to Machine Learning (ML) methods such as Support Vector Machines (SVM) and Artificial Neural Networks (ANN). In DL, hierarchical feature extraction is performed by deriving high-level features from lower-level features.

Researchers have conducted numerous studies in the past to diagnose COVID-19 based on Convolutional Neural Networks (CNN) to take advantage of DL. Most of these works use popular CNN architectures such as AlexNet, ResNet, Xception, etc. Wu et al. [18] presented a ResNet50 architecture-based algorithm to identify COVID-19 patients, and their accuracy rate was 76%. Ardakani et al. [19] presented a DL-based application using CT scan images to diagnose COVID-19. They benchmarked different CNN models trained on CT scan images with each other, and finally calculated that ResNet-101 and Xception models had 99.51% and 99.02% accuracy rates, respectively. These models had better accuracy than the other CNN models. Jaiswal et al. [20] developed a transfer learning-based application using the pre-trained Densenet 201 architecture. This CNN module classified COVID-19 and non-COVID-19 data with 96.21% accuracy. Wang et al. [21] stated that a clinical diagnosis can be achieved before pathogenic testing with AI techniques, and in this context, they conducted a study that analyzed changes in CT images of infected patients. For this, they modified the pre-trained Inception model. The overall accuracy was 89.66%. Sethy and Behera [22] extracted features using a large number of different pre-trained CNN models such as ResNet50, ResNet101, InceptionV3, GoogleNet, and VGG16. The authors then provided the classification with SVM. They stated that the ResNet-SVM structure provides high accuracy of 95.33%. Deng et al. [23] used five CNN models, including Xception, ResNet50, etc., to diagnose COVID-19 from chest X-ray and CT images. They achieved accuracies of 84% and 75% for Chest X-ray and CT scan images, respectively. Narin et al. [24] used CNN models, ResNet50, Inception-ResNetV2, InceptionV3, ResNet152, and ResNet101 for diagnosis of COVID-19-infected patients using chest X-ray images. The ResNet50 model gave the most successful classification accuracy according to the performance values obtained using five-fold cross-validation. Aslan et al. [13] performed a novel hybrid model to classify chest X-ray images as COVID-19, Viral Pneumonia, or Normal. For hybrid architecture, they combined modified AlexNet and Bidirectional Long Short-Term Memory (BiLSTM). At the end of the study, the authors stated that the hybrid architecture achieved 98.702% classification success. Mukherjee et al. [25] designed a CNN—tailored Deep Neural Network (DNN) that can collectively train and test both CT scans and chest X-ray images. In practice, the authors provided an overall accuracy of 96.28%. Aslan et al. [26] first performed lung segmentation with ANN for the detection of COVID-19 with CT images. They classified features extracted from segmented lung images with deep CNN models using different machine learning methods. They determined the parameters of each machine learning model

by hyperparameter optimization. At the end of the study, the authors stated that the highest accuracy was obtained with the DenseNet201-SVM structure, with an accuracy of 96.29%. Serte et al. [27] used a generative adversarial network (GAN) in addition to data augmentation to increase the number of CT samples in a small dataset. They then fed the images generated with data augmentation and GAN into different CNN models and performed COVID-19 detection. At the end of the study, 89% diagnostic accuracy was achieved.

It is possible to observe that previously made DL-based methods often have high classification success in detecting COVID-19. These studies are promising in terms of early COVID-19 detection, but many hyperparameters which belong to the DL network may increase also the success rate of the detection of infection. In literature, Artificial Bee Colony (ABC) [28], Bayesian Optimization [29], Tree Seed Algorithm (TSA) [30], and other optimization methods are used in various fields. These optimization techniques can tune hyperparameters in the deep network for a stronger prediction. However, for the detection of COVID-19, few studies have used optimization methods to improve current success. Ucar and Korkmaz [31] used Bayesian optimization to fine-tune the hyperparameters of the SqueezeNet CNN architecture, and as a result, they achieved a classification success of 98.3%. Nour et al. [32] designed a CNN model with five convolution layers for COVID-19 diagnosis. The deep-network features obtained with this CNN model were used to feed the ML algorithms, the k-nearest neighbor, SVM, and decision tree. The hyperparameters of the ML methods have been optimized using the Bayes optimization algorithm. As a result, the highest classification accuracy of 98.97% was obtained with SVM. Elaziz et al. [33] applied a modified Bayesian optimization algorithm together with an ML for the selection of useful features from CT images. Toğaçar et al. [34] used MobileNetV2 and SqueezeNet architectures to detect COVID-19. The most effective features were determined with the Social-Mimic Optimization method. Then, the features were fused and classified with the SVM algorithm, and their accuracy rate was 99.27%.

In this study, a DL-based COVID-19 detection system using CT-scans is proposed. A publicly available SARS-CoV-2 CT scan dataset [35,36] is used in this study. The dataset includes 1230 and 1252 CT scans of uninfected and infected patients, respectively. The application of COVID-19 detection can be addressed in two steps. The first step performs feature extraction and classification by modifying the pre-designed AlexNet architecture, as in many previous studies. The second step gives the extracted features to the optimized ANN classifier to improve the results in the first step. The ANN is trained by Tree Seed Algorithm (TSA) optimization method. In order to determine the best structure, various transfer functions and hidden layer neuron numbers are examined. The results prove that optimized ANN increases classification success.

The contributions of this study are listed as follows:

- A high-accuracy diagnosis of COVID-19 has been performed automatically.
- To improve the classification performance of end-to-end architectures, ANN is applied instead of fully connected layers.
- For a high classification performance, ANN is optimized by the TSA method.
- The proposed method can increase the diagnostic accuracy of previous studies using the CNN model.
- The applied experimental work outperforms many previous studies.

The remainder of the paper is organized as follows. In Section 2, the dataset and suggested methods are explained in detail. Section 3 contains the results of the proposed method. Section 4 discusses the proposed method and makes comparisons with previous studies. Finally, Section 5 concludes the work overall and provides information about future work.

2. Materials and Methods

This section provides detailed information about the dataset, TSA optimization, mAlexNet architecture, and the proposed hybrid model.

2.1. SARS-CoV-2 Ct-Scan Dataset

In this study, a publicly available dataset called SARS-CoV-2 Ct-Scan Dataset [35,36] is used due to having large numbers of data and the ability to compare previous studies done with this dataset. Five researchers from Lancaster University United Kingdom and Public Hospital of the Government Employees of Sao Paulo created this dataset with 1252 infected patients' CT scans and 1230 uninfected patients' CT scans in May 2020. There are a totally of 2482 CT scans in the dataset. The data in this dataset were generated by collecting asymmetrical CT scans of real patients in hospitals in Sao Paulo, Brazil. CT scans of two patients with positive and negative diagnosis of COVID-19 are shown in Figure 1.

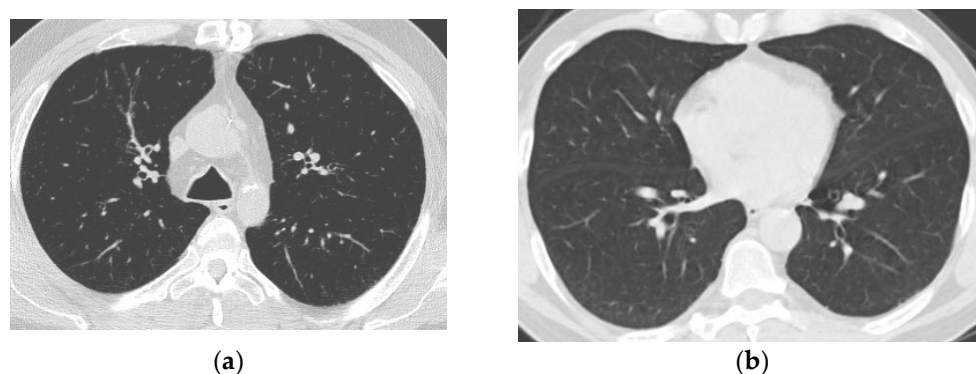


Figure 1. Positive and negative images in the SARS-CoV-2 Ct-Scan dataset. (a) CT scan of a patient infected with COVID-19; (b) CT scan of a patient not infected with COVID-19.

2.2. The Tree Seed Algorithm (TSA)

The TSA algorithm is based on natural phenomena between trees and their spread seeds. The land where trees are grown is assumed as search space. Each tree is a solution candidate for the problem to be optimized. The seeds are produced by the trees in order to grow a new tree, which is going to be a candidate for the solution of the problem. The purpose of the optimization process is to generate new coordinates of the seeds using the available information. Two equations used for this purpose are presented in Equations (1) and (2) [30].

$$S_{ij} = T_{ij} + \alpha_{ij} \times (B_j - T_{rj}) \quad (1)$$

$$S_{ij} = T_{ij} + \alpha_{ij} \times (T_{ij} - T_{rj}) \quad (2)$$

In Equations (1) and (2), S_{ij} represents the j th dimension of i th seed and T_{ij} is the j th dimension of the i th tree. B_j is the j th dimension of the best tree ever found. T_{rj} is the j th dimension of the r th tree, which is randomly selected from the population. α is the scaling factor which is randomly produced between 1 and -1 . In seed production, two equations are presented, thus there has to be a criterion that determines which equation will be used. This is controlled by the search tendency (ST) parameters in the range of 0 to 1. While the higher value of ST makes the algorithm condense on local solutions, the lower ST value forces it to make a global search. Although the number of seeds produced by a single tree was completely random, TSA's performance analysis determined that TSA performed best when the number of seeds produced by each tree was between 10% and 25% of the population size [30].

In the initial of the algorithm, the optimization parameters are created randomly in a range of specific upper and lower bounds for each parameter. Then, for each dimension of each seed of each tree in the population, Equation (1) or Equation (2) is randomly applied and new seeds are created. The termination criteria are checked each iteration. These criteria may be the number of iteration limits, error threshold or no change in error, etc. When termination criteria are met, the best result in the population is reported. The flowchart of TSA is presented in Figure 2.

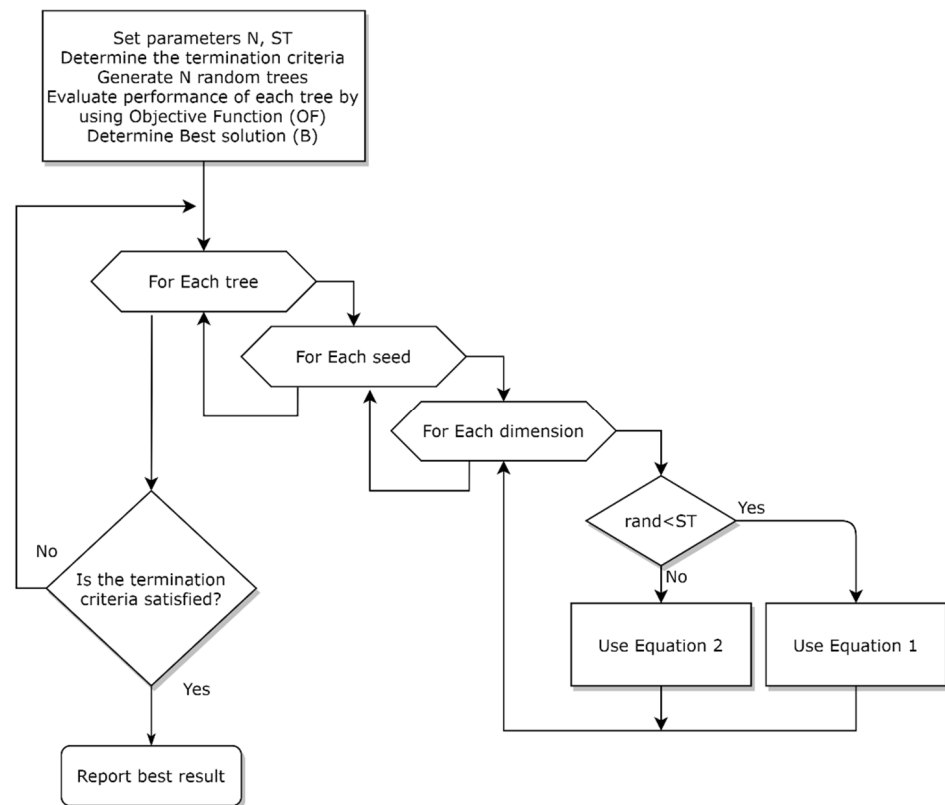


Figure 2. Flow diagram of Tree Seed Algorithm.

2.3. Proposed mAlexNet Architecture

Due to the high performance of CNNs in various image recognition applications, they are highly preferred [37,38]. In this study, to classify the CT-scan images, a modified AlexNet (mAlexNet) created by using transfer learning is used. AlexNet is made up of 25 layers together with a convolution layer, Rectified Linear Unit (ReLU), fully connected (fc) layer, normalization layer, pooling layer, etc. The three layers at the end of the AlexNet model have been slightly modified (fine-tuning) to be compatible with existing study inputs. In order to distinguish whether a CT image shows COVID-19 or not, these final three layers are removed. Other parameters of the pre-trained AlexNet architecture are retained. Instead of the removed layers, new layers suitable for this study are added, as in Figure 3. This new architecture is called the modified AlexNet (mAlexNet). In the fc8 layer of pre-trained AlexNet, the number of the neurons is 1000. The number of features used for classification in our application is 25. Therefore, the number of neurons in the fc8 layer is changed to 25 in the mAlexNet architecture. In Figure 3, the mAlexNet structure is presented. Table 1 shows the layer parameters and training options of mAlexNet. When the training options are examined, it can be realized that the Mini Batch parameter, which provides the training data to be divided into smaller parts, is 40. The optimization algorithm Stochastic Gradient Descent with Momentum (SGDM) is applied to reduce the training error. Parameters of the SGDM algorithm are also shown in Table 1.

$$\theta_{l+1} = \theta_l - \alpha \nabla E(\theta_l) + \gamma(\theta_l - \theta_{l-1}) \quad (3)$$

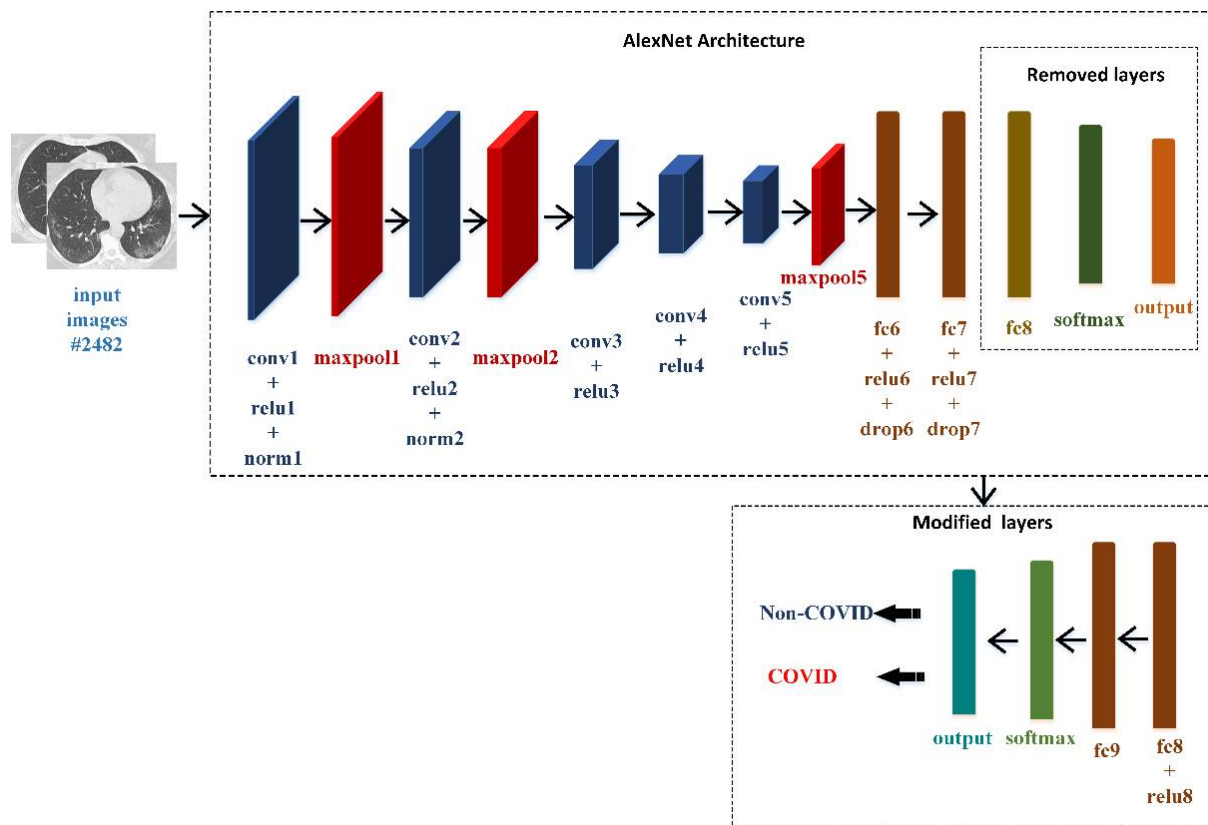


Figure 3. mAlexnet model.

Table 1. mAlexnet layer parameters and training options.

Layer Name	Size	Filter Size	Stride	Padding	Output Channel	Activation Function
conv1	55 × 55	11 × 11	4	0	96	relu
maxpool1	27 × 27	3 × 3	2	0	96	-
conv2	27 × 27	5 × 5	1	2	256	relu
maxpool2	13 × 13	3 × 3	2	0	256	-
conv3	13 × 13	3 × 3	1	1	384	relu
conv4	13 × 13	3 × 3	1	1	384	relu
conv5	13 × 13	3 × 3	1	1	256	relu
maxpool5	6 × 6	3 × 3	2	0	256	-
fc6	-	-	-	-	4096	relu
fc7	-	-	-	-	4096	relu
fc8	-	-	-	-	25	relu
fc9	-	-	-	-	2	softmax

Training Options				
Optimization Alg.	Maximum Epoch	Mini Batch Size	Initial Learning Rate (α)	Momentum (γ)
SGDM	25	40	0.001	0.95

With SGDM, the weights of the network are updated according to the estimation error. Equation (3) is used to update the weights. With this equation, the weights are updated according to the loss function ($E(\theta_l)$). In order for the error value to decrease after each update, the loss function is moved in the direction of the negative gradient. The speed of this movement depends on the learning rate (α). The contribution of the current weight value to the weight value in the previous iteration is determined by the Momentum (γ) coefficient. The values of α and γ parameters in Equation (3) are shown in Table 1.

2.4. Proposed TSA-ANN Model

This section discusses the classification of mAlexNet features using TSA-optimized ANN (TSA-ANN). The mAlexNet architecture described in the previous section is com-

bined with the TSA-ANN structure as in Figure 4. 25; features extracted via mAlexNet are given to the TSA-ANN structure for classification.

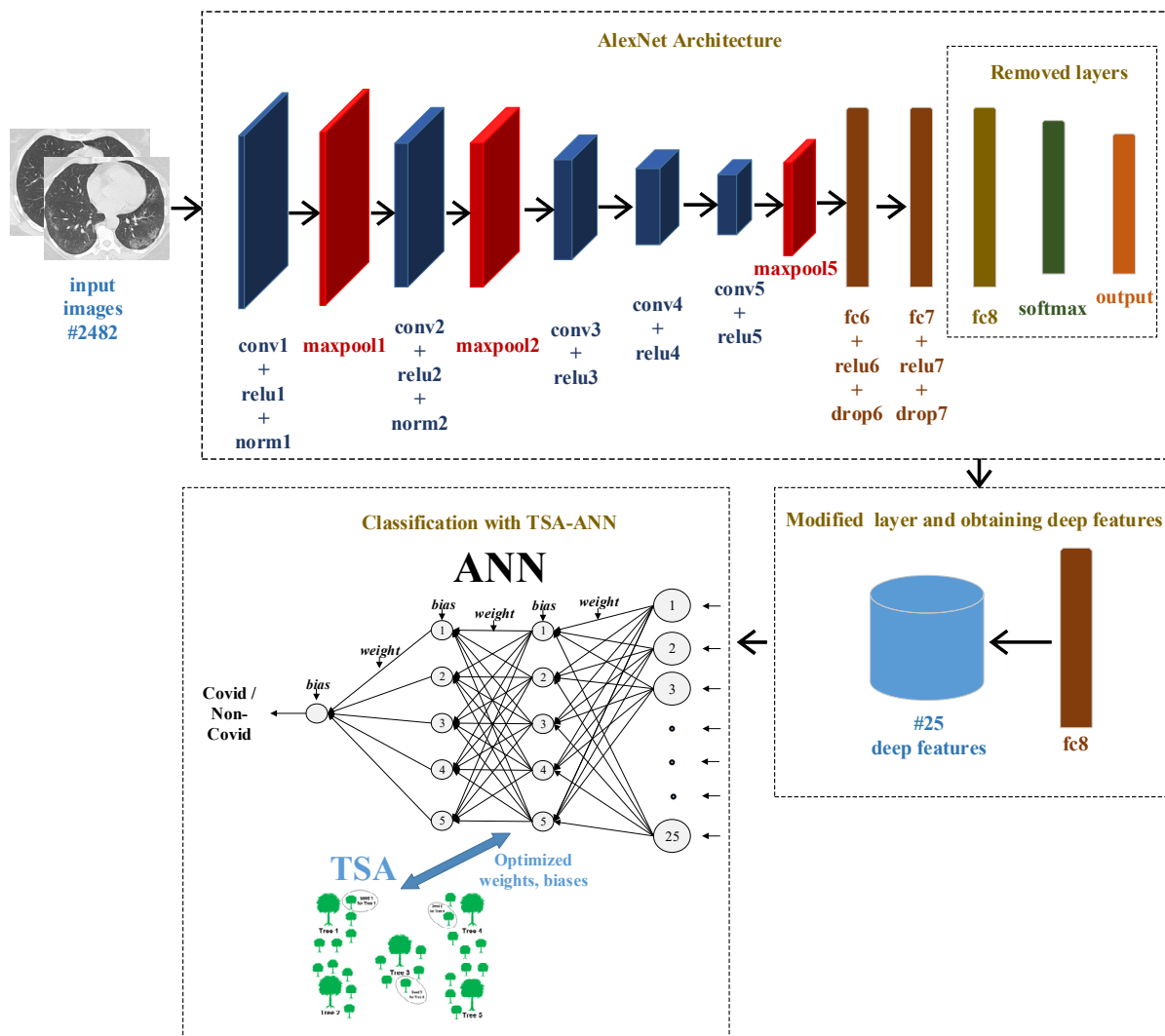


Figure 4. mAlexNet—TSA-ANN model.

The proposed ANN model consists of an input layer, two hidden layers, and an output layer. In the input layer, there are 25 neurons. It is also the same as the size of the input features. The number of neurons in both hidden layers is determined to be five by the trial and error method. The output layer has a single neuron.

The activation functions used in the neural network are Hyperbolic Tangent Sigmoid and Logarithmic Sigmoid functions. Since the range of the output layer is [0 1], the activation function of the output layer is determined to be a Logarithmic Sigmoid function. The activation functions of hidden layers are determined to be Hyperbolic Tangent Sigmoid functions by the trial and error method. The Logarithmic Sigmoid and Hyperbolic Tangent Sigmoid functions are presented in Equations (4) and (5), respectively.

$$AF(x) = \frac{1}{1 + e^{-x}} = \text{logsig}(x) \tag{4}$$

$$AF(x) = \frac{e^x - e^{-x}}{e^x + e^{-x}} = \text{tansig}(x) \tag{5}$$

The applied input data are transferred to each neuron in the first hidden layer by multiplying the corresponded coefficient $W_{(k,i,j)}$. The (k, i, j) indexes indicate the connection coefficient in the k th layer, between i th data and j th neuron. For each neuron, there is also a bias value represented by $B_{(k,j)}$ symbol. Then, the sum all of the inputs to a neuron is applied to an Activation Function (AF). The result of this function is the value of the neuron. This value of the j th neuron in the k th layer $V_{(k,j)}$ can be calculated by the following formula:

$$V_{(k,j)} = AF \left(\sum_{i=1}^{N_{k-1}} V_{(k-1,i)} W_{(k,i,j)} + B_{(k,j)} \right) \quad (6)$$

where the N_{k-1} is the number of neurons in the $(k - 1)$ th layer. As seen from the formula, in each layer, there are $N_{k-1} * N_k$ W parameters and N_k B parameters. Thus, the total number of parameters that need to be optimized is $(N_{k-1} + 1) * N_k$. In Table 2, the number of neurons, activation functions, and parameter count of each layer are presented.

Table 2. Neural network properties.

Layers	Number of Neurons	Activation Function	Parameter Count
Layer 1 (Input Layer)	25	-	-
Layer 2 (1st Hidden Layer)	5	Hyperbolic Tangent Sigmoid	130
Layer 3 (2st Hidden Layer)	5	Hyperbolic Tangent Sigmoid	30
Layer 4 (Output Layer)	1	Logarithmic Sigmoid	6

As presented in Table 2, the weight and bias values of each layer after the input layer of the ANN are optimized with TSA. This optimization process can be thought of as the training phase of the network. For example, $25 \times 5 + 5 = 130$ parameters for Layer 2, $5 \times 5 + 5 = 30$ parameters for Layer 3 and $5 \times 1 + 1 = 6$ parameters for the output layer should be optimized. This optimization process aims to minimize the error value. Therefore, the objective function is related to the error between the target value and the predicted value. A total of 166 network parameters need to be optimized for the training of the network. During this period, the training dataset is used. The Mean Absolute Error (MAE) (see Equation (7)) for the training dataset generated by the ANN with network parameters is used as the objective function of TSA optimization. The n , y , and \hat{y} in Equation (7) represent the number of data, the actual output value, and the estimated output value, respectively. During the optimization, the error value is reduced in each iteration. After the optimization is completed, the ANN is updated with the determined parameters. This ANN is called a trained ANN from now on. The performance of the trained ANN is determined by using a test dataset. These results are presented in detail in Section 3.

$$MAE = \frac{1}{n} \sum |y - \hat{y}| \quad (7)$$

3. Results

The performance of both architectures expressed above is calculated by using a test dataset. Both architectures are created with the architectural parameters specified in Table 1. Training and testing of the methods developed within the scope of this application are carried out on a laptop computer with Intel Core i7-7700HG CPU, NVIDIA GeForce GTX 1050 4 GB, 16 GB RAM. Firstly, 80% of the COVID-19 dataset is used in the training of the mAlexNet structure in Figure 3. The training graph is successfully obtained as seen in Figure 5. Then, the performance of mAlexNet is tested with the remaining 20% of the dataset, called the test dataset.

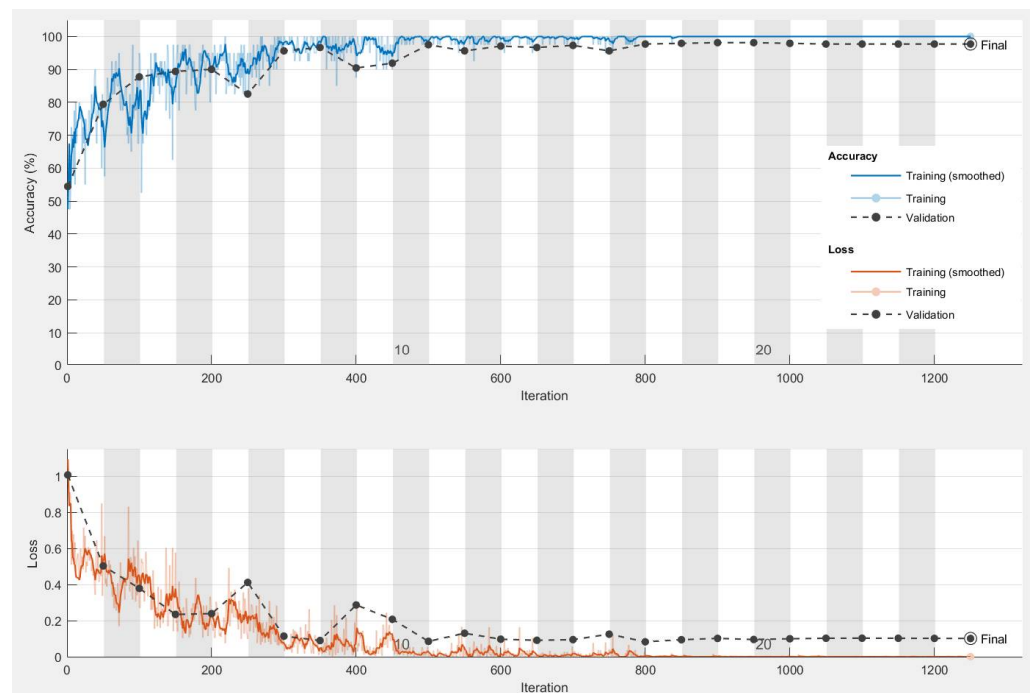


Figure 5. Training graphics of mAlexNet model.

Figure 6 shows the confusion matrix of mAlexNet and TSA-ANN implementations. Figure 6a is the confusion matrix obtained by classifying test data with mAlexNet. Figure 6b is the confusion matrix obtained as a result of the application that enables classification of mAlexNet features with the optimized ANN (TSA-ANN) structure. The parameters used for the optimization algorithm in the TSA-ANN application are as follows: population size: 50, number of iterations: 1000, and search tendency: 0.1. When both confusion matrices are examined, it is seen that COVID-19 infected scans with asymmetrical patterns are more successfully diagnosed with the TSA-ANN structure. Additionally, various performance metrics such as accuracy, specificity, MCC, F1-score, recall, and precision are calculated and presented. For each metric, formulations are given between Equations (8)–(13) [13,39,40]. These metrics prove the robustness and unbiasedness of the classification performance obtained as a result of the proposed method. Table 3 shows the results for these performance metrics. According to Table 3, both applications are successful in detecting COVID-19 infection using CT scans. But the performance of the hybrid TSA-ANN added mAlexNet model is better than the single mAlexNet structure in terms of accuracy. The accuracy rates of models are 97.92% and 98.54% for mAlexNet and mAlexNet + TSA-ANN, respectively. Additionally, Precision, Sensitivity, F1-Score, MCC, and Specificity indicators are also better in hybrid architecture, as seen in Table 3. It is possible to conclude that deep architecture using the TSA-ANN classification has better performance and unbiased classification.

$$\text{Accuracy} = \frac{tp + tn}{tp + fp + tn + fn} \times 100 \quad (8)$$

$$\text{Sensitivity} = \frac{tp}{tp + fn} \quad (9)$$

$$\text{Specificity} = \frac{tn}{tn + fp} \quad (10)$$

$$\text{Precision} = \frac{tp}{tp + fp} \quad (11)$$

$$\text{F1-score} = \frac{2tp}{2tp + fp + fn} \quad (12)$$

$$MCC = \frac{(tp * tn) - (fn * fp)}{\sqrt{(tp + fn) * (tn + fp) * (tp + fp) * (tn + fn)}} \tag{13}$$

tp: True Positive
tn: True Negative
fp: False Positive
fn: False Negative

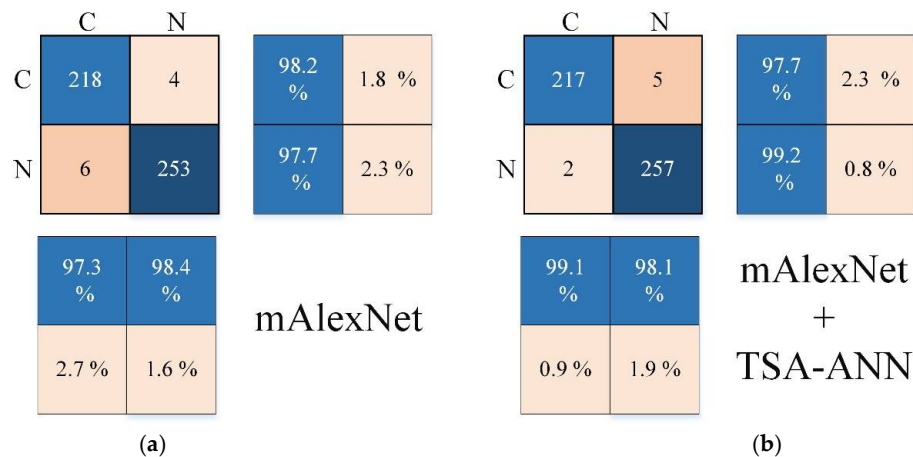


Figure 6. Confusion matrices of proposed models. (a) mAlexNet; (b) mAlexNet + TSA-ANN.

Table 3. Performance metrics of the proposed models.

Model	Accuracy	Sensitivity	Specificity	Precision	F1-Score	MCC
mAlexNet	97.92	0.9820	0.9768	0.9732	0.9776	0.9582
mAlexNet + TSA-ANN	98.54	0.9775	0.9923	0.9909	0.9841	0.9708

To prove the robustness of the proposed method, the same application is also performed on a different dataset. For this, the COVID-19 Radiology database [17] is preferred. Only the COVID-19 and Normal classes in this dataset are used. However, the data numbers in this dataset are unbalanced. The number of COVID-19 classes is 219, while the Normal (non-COVID) class number is 1341. Therefore, first, data augmentation is applied for the class with few data, resulting in a total number of images of 2436. 80% of all data is allocated as training and 20% as testing. Figure 7 shows the confusion matrices obtained after applying the proposed method on the COVID-19 Radiology database. Figure 7a is provided by mAlexNet and average accuracy is 99.38%. Figure 7b is provided by mAlexNet-TSA-ANN with an average accuracy of 99.59%. The results show that the proposed method is also effective in different datasets.

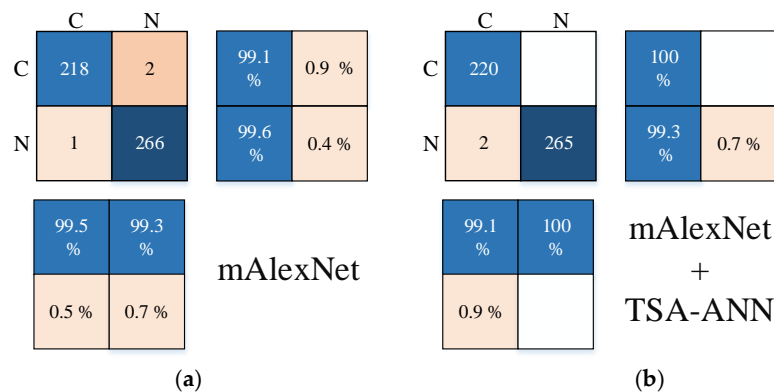


Figure 7. Confusion matrices of proposed models on COVID-19 Radiology database. (a) mAlexNet; (b) mAlexNet + TSA-ANN.

4. Discussion

Many DL-based diagnostic methods developed so far have directly used CNN models. However, different techniques can be used to improve the performance obtained with a CNN model. The aim of this study is to show that the mAlexNet–TSA-ANN hybrid structure is highly effective in detecting COVID-19. Moreover, this experiment was implemented on AlexNet, which is simpler than other CNN models. The results showed that even a fine-tuned AlexNet (mAlexNet) combined with the TSA-ANN method outperforms many studies. Some of the previous studies suggesting different DL-based methods are shown in Table 4. According to Table 4, it is seen that the proposed mAlexNet–TSA-ANN structure is superior to previous studies using the same dataset.

Table 4. Benchmarking of the proposed mAlexNet-TSA-ANN with previous studies.

Study	Method	Accuracy (%)
Soares et al. [41]	xDNN	97.38%
Özkaya et al. [42]	CNN + SVM	94.03%
Tetila et al. [43]	Inception-Resnet-v2	98.4%
Panwar et al. [44]	Color Visualization (Grad-CAM)	95%
Wang et al. [45]	Contrastive Learning	90.83 ± 0.93
Jaiswal et al. [20]	DenseNet201	96.25%
Öztürk et al. [46]	WOA-MLP	88.06%
Silva et al. [47]	EfficientNet	98.50%
Yazdani et al. [48]	Attentional Convolutional Network	92%
Proposed approach	mAlexNet—TSA-ANN	98.54%

Although the proposed method is superior to previous studies in terms of accuracy, it has some limitations. The most important limitation is that the developed optimization approach slows down the training process of the network. Only the mAlexNet structure realizes faster training. Another limitation is that the TSA optimization method used also needs parameter optimization. In addition, the results obtained are valid only for the datasets used. Its success on other different datasets is unpredictable. For a general success, a study should be done that includes all different datasets.

5. Conclusions

Early detection of COVID-19 disease is crucial due to the high rate of spread among humans. This study uses computed tomography (CT) images to quickly and accurately diagnose COVID-19. Both proposed models include the AlexNet architecture. In the first model, mAlexNet architecture is created and classification is performed. In the second model, 25 features extracted from each image with mAlexNet are given to the TSA-optimized ANN for classification. The different aspect of this study compared to other studies is the use of the TSA-ANN-based hybrid model. The high accuracy achieved with the hybrid architecture shows that the model is a powerful classifier. By feeding the trained hybrid architecture with CT images, COVID-19 can be detected quickly. In future studies, to increase the success of the system, the lungs will be determined from the CT images by applying semantic segmentation. Then, the number of images will be increased with the obtained lung images through data enhancement methods. It is planned to achieve higher accuracy by testing different architectures with these images.

Author Contributions: M.F.A.: Investigation and writing—reviewing and editing. K.S.: Investigation, methodology, supervision. E.R.: Investigation and supervision, editing. All authors have read and agreed to the published version of the manuscript.

Funding: This research received no external funding.

Institutional Review Board Statement: Not applicable.

Informed Consent Statement: Not applicable.

Data Availability Statement: The dataset is cited in the manuscript. The data access link is <https://www.kaggle.com/datasets/plameneduardo/sarscov2-ctscan-dataset> (accessed on 10 May 2022).

Conflicts of Interest: The authors declare no conflict of interest.

References

- Green, A. Li wenliang. *Lancet* **2020**, *395*, 682. [CrossRef]
- Khan, A.I.; Shah, J.L.; Bhat, M.M. Coronet: A deep neural network for detection and diagnosis of COVID-19 from chest X-ray images. *Comput. Methods Programs Biomed.* **2020**, *196*, 105581. [CrossRef]
- Mahase, E. Coronavirus: COVID-19 has killed more people than SARS and MERS combined, despite lower case fatality rate. *BMJ* **2020**, *368*, m641. [CrossRef]
- Spinelli, A.; Pellino, G. COVID-19 pandemic: Perspectives on an unfolding crisis. *Br. J. Surg.* **2020**, *107*, 785–787. [CrossRef]
- WHO. *Coronavirus Disease 2019 (COVID-19) Situation Report—51, 11 March 2020*; WHO: Geneva, Switzerland, 2020.
- Thakur, N.; Han, C.Y. An Exploratory Study of Tweets about the SARS-CoV-2 Omicron Variant: Insights from Sentiment Analysis, Language Interpretation, Source Tracking, Type Classification, and Embedded URL Detection. *Preprints* **2022**, 2022050238. [CrossRef]
- JH. COVID-19 Map—Johns Hopkins Coronavirus Resource Center. Available online: <https://coronavirus.jhu.edu/map.html> (accessed on 10 June 2022).
- Guan, W.-J.; Ni, Z.-Y.; Hu, Y.; Liang, W.-H.; Ou, C.-Q.; He, J.-X.; Liu, L.; Shan, H.; Lei, C.-L.; Hui, D.S. Clinical characteristics of coronavirus disease 2019 in China. *N. Engl. J. Med.* **2020**, *382*, 1708–1720. [CrossRef]
- Jiang, Y.; Chen, H.; Loew, M.; Ko, H. COVID-19 CT Image Synthesis with a Conditional Generative Adversarial Network. *arXiv* **2020**, arXiv:2007.14638. [CrossRef]
- Jawerth, N. How is the COVID-19 virus detected using real time RT-PCR. *IAEA Bull.* **2020**, *61*, 8–11.
- Ai, T.; Yang, Z.; Hou, H.; Zhan, C.; Chen, C.; Lv, W.; Tao, Q.; Sun, Z.; Xia, L. Correlation of chest CT and RT-PCR testing in coronavirus disease 2019 (COVID-19) in China: A report of 1014 cases. *Radiology* **2020**, *296*, 200642. [CrossRef] [PubMed]
- Fang, Y.; Zhang, H.; Xie, J.; Lin, M.; Ying, L.; Pang, P.; Ji, W. Sensitivity of chest CT for COVID-19: Comparison to RT-PCR. *Radiology* **2020**, *296*, 200432. [CrossRef]
- Aslan, M.F.; Unlarsen, M.F.; Sabanci, K.; Durdu, A. CNN-based transfer learning-BiLSTM network: A novel approach for COVID-19 infection detection. *Appl. Soft Comput.* **2020**, *98*, 106912. [CrossRef] [PubMed]
- Barello, S.; Palamenghi, L.; Graffigna, G. Stressors and Resources for Healthcare Professionals during the COVID-19 Pandemic: Lesson Learned From Italy. *Front. Psychol.* **2020**, *11*, 2179. [CrossRef] [PubMed]
- Chen, X.; Li, J.; Zhang, Y.; Lu, Y.; Liu, S. Automatic feature extraction in X-ray image based on deep learning approach for determination of bone age. *Future Gener. Comput. Syst.* **2020**, *110*, 795–801. [CrossRef]
- Kieu, P.N.; Tran, H.S.; Le, T.H.; Le, T.; Nguyen, T.T. Applying multi-CNNs model for detecting abnormal problem on chest X-ray images. In Proceedings of the 2018 10th International Conference on Knowledge and Systems Engineering (KSE), Ho Chi Minh City, Vietnam, 1–3 November 2018; pp. 300–305.
- Chowdhury, M.E.; Rahman, T.; Khandakar, A.; Mazhar, R.; Kadir, M.A.; Mahbub, Z.B.; Islam, K.R.; Khan, M.S.; Iqbal, A.; Al Emadi, N. Can AI help in screening viral and COVID-19 pneumonia? *IEEE Access* **2020**, *8*, 132665–132676. [CrossRef]
- Wu, X.; Hui, H.; Niu, M.; Li, L.; Wang, L.; He, B.; Yang, X.; Li, L.; Li, H.; Tian, J. Deep learning-based multi-view fusion model for screening 2019 novel coronavirus pneumonia: A multicentre study. *Eur. J. Radiol.* **2020**, *128*, 109041. [CrossRef]
- Ardakani, A.A.; Kanafi, A.R.; Acharya, U.R.; Khadem, N.; Mohammadi, A. Application of deep learning technique to manage COVID-19 in routine clinical practice using CT images: Results of 10 convolutional neural networks. *Comput. Biol. Med.* **2020**, *121*, 103795. [CrossRef]
- Jaiswal, A.; Gianchandani, N.; Singh, D.; Kumar, V.; Kaur, M. Classification of the COVID-19 infected patients using DenseNet201 based deep transfer learning. *J. Biomol. Struct. Dyn.* **2021**, *39*, 5682–5689. [CrossRef]
- Wang, S.; Kang, B.; Ma, J.; Zeng, X.; Xiao, M.; Guo, J.; Cai, M.; Yang, J.; Li, Y.; Meng, X.; et al. A deep learning algorithm using CT images to screen for Corona virus disease (COVID-19). *Eur. Radiol.* **2021**, *31*, 6096–6104. [CrossRef]
- Sethy, P.K.; Behera, S.K. Detection of Coronavirus Disease (COVID-19) Based on Deep Features. *Preprints* **2020**, 2020030300. [CrossRef]
- Deng, X.; Shao, H.; Shi, L.; Wang, X.; Xie, T. A classification–detection approach of COVID-19 based on chest X-ray and CT by using keras pre-trained deep learning models. *Comput. Model. Eng. Sci.* **2020**, *125*, 579–596. [CrossRef]
- Narin, A.; Kaya, C.; Pamuk, Z. Automatic detection of coronavirus disease (COVID-19) using X-ray images and deep convolutional neural networks. *arXiv* **2020**, arXiv:2003.10849. [CrossRef] [PubMed]
- Mukherjee, H.; Ghosh, S.; Dhar, A.; Obaidullah, S.M.; Santosh, K.; Roy, K. Deep neural network to detect COVID-19: One architecture for both CT Scans and Chest X-rays. *Appl. Intell.* **2021**, *51*, 2777–2789. [CrossRef]
- Aslan, M.F.; Sabanci, K.; Durdu, A.; Unlarsen, M.F. COVID-19 diagnosis using state-of-the-art CNN architecture features and Bayesian Optimization. *Comput. Biol. Med.* **2022**, *142*, 105244. [CrossRef] [PubMed]
- Serte, S.; Dirik, M.A.; Al-Turjman, F. Deep Learning Models for COVID-19 Detection. *Sustainability* **2022**, *14*, 5820. [CrossRef]

28. Karaboga, D.; Basturk, B. A powerful and efficient algorithm for numerical function optimization: Artificial bee colony (ABC) algorithm. *J. Glob. Optim.* **2007**, *39*, 459–471. [[CrossRef](#)]
29. Frazier, P.I. A tutorial on bayesian optimization. *arXiv* **2018**, arXiv:1807.02811.
30. Kiran, M.S. TSA: Tree-seed algorithm for continuous optimization. *Expert Syst. Appl.* **2015**, *42*, 6686–6698. [[CrossRef](#)]
31. Ucar, F.; Korkmaz, D. COVIDiagnosis-Net: Deep Bayes-SqueezeNet based Diagnostic of the Coronavirus Disease 2019 (COVID-19) from X-ray Images. *Med. Hypotheses* **2020**, *140*, 109761. [[CrossRef](#)]
32. Nour, M.; Cömert, Z.; Polat, K. A novel medical diagnosis model for COVID-19 infection detection based on deep features and Bayesian optimization. *Appl. Soft Comput.* **2020**, *97*, 106580. [[CrossRef](#)]
33. Elaziz, M.A.; Hosny, K.M.; Salah, A.; Darwish, M.M.; Lu, S.; Sahlol, A.T. New machine learning method for image-based diagnosis of COVID-19. *PLoS ONE* **2020**, *15*, e0235187. [[CrossRef](#)]
34. Toğaçar, M.; Ergen, B.; Cömert, Z. COVID-19 detection using deep learning models to exploit Social Mimic Optimization and structured chest X-ray images using fuzzy color and stacking approaches. *Comput. Biol. Med.* **2020**, *121*, 103805. [[CrossRef](#)] [[PubMed](#)]
35. Angelov, P.; Almeida Soares, E. SARS-CoV-2 CT-Scan Dataset. Available online: <https://www.kaggle.com/plameneduardo/sarscov2-ctscan-dataset> (accessed on 10 June 2022).
36. Angelov, P.; Almeida Soares, E. Explainable-by-Design Approach for COVID-19 Classification via CT-Scan. *medRxiv* **2020**. Available online: <https://www.medrxiv.org/content/10.1101/2020.04.24.20078584v1> (accessed on 10 June 2022).
37. Krizhevsky, A.; Sutskever, I.; Hinton, G.E. Imagenet classification with deep convolutional neural networks. *Commun. ACM* **2017**, *60*, 84–90. [[CrossRef](#)]
38. Simonyan, K.; Zisserman, A. Very deep convolutional networks for large-scale image recognition. *arXiv* **2014**, arXiv:1409.1556.
39. Aslan, M.F.; Sabanci, K.; Durdu, A. A CNN-based novel solution for determining the survival status of heart failure patients with clinical record data: Numeric to image. *Biomed. Signal Process. Control* **2021**, *68*, 102716. [[CrossRef](#)]
40. Sabanci, K.; Aslan, M.F.; Ropelewska, E.; Unlarsen, M.F. A convolutional neural network-based comparative study for pepper seed classification: Analysis of selected deep features with support vector machine. *J. Food Process Eng.* **2021**, *45*, e13955. [[CrossRef](#)]
41. Soares, E.; Angelov, P.; Biaso, S.; Froes, M.H.; Abe, D.K. SARS-CoV-2 CT-Scan Dataset: A Large Dataset of Real Patients CT Scans for SARS-CoV-2 Identification. *medRxiv* **2020**. Available online: <https://www.medrxiv.org/content/10.1101/2020.04.24.20078584v3> (accessed on 10 June 2022).
42. Özkaya, U.; Öztürk, Ş.; Budak, S.; Melgani, F.; Polat, K. Classification of COVID-19 in Chest CT Images using Convolutional Support Vector Machines. *arXiv* **2020**, arXiv:2011.05746.
43. Tetila, E.; Bressen, K.; Astolfi, G.; Sant’Ana, D.A.; Pache, M.C.; Pistori, H. System for quantitative diagnosis of COVID-19-associated pneumonia based on superpixels with deep learning and chest CT. *Res. Sq.* **2020**. [[CrossRef](#)]
44. Panwar, H.; Gupta, P.K.; Siddiqui, M.K.; Morales-Menendez, R.; Bhardwaj, P.; Singh, V. A deep learning and grad-CAM based color visualization approach for fast detection of COVID-19 cases using chest X-ray and CT-Scan images. *Chaos Solitons Fractals* **2020**, *140*, 110190. [[CrossRef](#)]
45. Wang, Z.; Liu, Q.; Dou, Q. Contrastive cross-site learning with redesigned net for COVID-19 CT classification. *IEEE J. Biomed. Health Inform.* **2020**, *24*, 2806–2813. [[CrossRef](#)]
46. Öztürk, Ş.; Yigit, E.; Özkaya, U. Fused Deep Features Based Classification Framework for COVID-19 Classification with Optimized MLP. *Selçuk Univ. J. Eng. Sci. Technol.* **2020**, *8*, 15–27.
47. Silva, P.; Luz, E.; Silva, G.; Moreira, G.; Silva, R.; Lucio, D.; Menotti, D. COVID-19 detection in CT images with deep learning: A voting-based scheme and cross-datasets analysis. *Inform. Med. Unlocked* **2020**, *20*, 100427. [[CrossRef](#)] [[PubMed](#)]
48. Yazdani, S.; Minaee, S.; Kafieh, R.; Saedizadeh, N.; Sonka, M. COVID CT-net: Predicting COVID-19 from chest CT images using attentional convolutional network. *arXiv* **2020**, arXiv:2009.05096.